Carbohydrate Polymers 96 (2013) 426–434

Contents lists available at SciVerse ScienceDirect

Carbohydrate Polymers

journal homepage: www.elsevier.com/locate/carbpol

Ultra-small and anionic starch nanospheres: Formation and vitro thrombolytic behavior study

Yinjuan Huang[a], Shenglong Ding[a], Mingzhu Liu[a,*], Chunmei Gao[a], Jinlong Yang[a], Xinjie Zhang[a], Bin Ding[b]

[a] Key Laboratory of Nonferrous Metal Chemistry and Resources Utilization of Gansu Province, State Key Laboratory of Applied Organic Chemistry and Department of Chemistry, Lanzhou University, Lanzhou 730000, PR China
[b] Zhengzhou Research Institute for Abrasives and Grinding, Zhengzhou 450006, PR China

ARTICLE INFO

Article history:
Received 8 February 2013
Received in revised form 8 April 2013
Accepted 9 April 2013
Available online 18 April 2013

Keywords:
Anionic starch nanospheres
Soluble starch
Thrombolytic behavior
NK

ABSTRACT

This paper is considered as the first report on the investigation of nattokinase (NK) release from anionic starch nanospheres. The ultra-small and anionic starch nanospheres were prepared by the method of reverse micro-emulsion crosslinking in this work. Starch nanospheres were characterized through Fourier transform infrared (FTIR) spectroscopy, scanning electron microscopy (SEM), transmission electron microscopy (TEM) and dynamic light scattering (DLS). Effects of preparation conditions on particle size were studied. The cytotoxicity, biodegradable and vitro thrombolytic behaviors of nattokinase (NK) loaded anionic starch nanospheres were also studied. The results showed that the anionic starch nanospheres are non-toxic, biocompatible and biodegradable. Moreover, the anionic starch nanospheres can protect NK from fast biodegradation hence prolongs the circulation in vivo and can reduce the risk of acute hemorrhage complication by decreasing the thrombolysis rate.

1. Introduction

As a source of stored energy, starch is a naturally occurring polysaccharide produced by many plants and composed of two different components linear amylose and branched amylopectin. Normally, amylose account for 20–30% and amylopectin account for 70–80% of starch, respectively, which depend on the species of source. Due to many attractive properties of starch, such as economy, abundant, renewable, innocuity, biodegradability, biocompatibility and the capacity to bind with a wide variety of molecules via physical and chemical interaction (Li & Ni, 2004; Polaczek, Malenki, & Tomasik, 2000), starch can be used as biocompatible materials (Jobling, 2004; Song, Zhao, Dong, & Deng, 2009). Whereas, the big size of native starch particles restricts their applications in many field (Angellier, Molina-Boisseau, & Dufresne, 2005; Kristo & Biliaderis, 2007; Valodkar & Thakore, 2011), especially in medical field (Chen et al., 2008; Simi & Emilia Abraham, 2007; Thielemans, Belgacem, & Dufresne, 2006). Starch nanoparticles have many advantages as a delivery material, such as convenience of modifying surface properties, controlling particle size and release of pharmacologically active agents, less toxic, to achieve the targeting action of the drug at the therapeutically optimal rate and dose regimen. Recently, a widely summarized review on starch nanoparticle preparation, characterization, and applications has been published (Le Corre, Bras, & Dufresne, 2010). Starch nanoparticles have been prepared via reactive extrusion, regioselective modification and precipitation (Angellier et al., 2005; Kim & Lim, 2009; Ma, Peter, & Yu, 2008; Song, Thio, & Deng, 2011), respectively. The starch nanoparticles display a spherical or oval shape, with diameters in the range of 10–200 nm.

Recently, thrombotic diseases does harm to the life and health of human severely, especially, heart and cerebral thrombolic disease is one of the most important and common diseases that are harmful to the health of aged people. Herein, the studies of thrombolytic drugs have been paid attention in the world. Currently, nattokinase (NK) that can dissolve fibrin directly is high efficient, secure and economic, thus became the focus of the studies of thrombolytic drugs. Although NK possess a high fibrinolytic efficiency, an increased blood drug concentration of the free NK will cause serious side-effects such as hemorrhage (Brekenfeld et al., 2007). On the other hand, protein is flimsy in vivo due to fast clearance by enzymes like proteinase (Erdoğan, Özer, & Bilgili, 2005). To find a way to minimize side effects of NK, improve their stability and lengthen their circulation time for the treatment of thrombotic diseases holds great promise. Ultra-small systems are more ideal for the thrombolysis therapy because drugs have to be delivered to the thrombus through the narrow residual blood flow channels around the arterial obstruction (Francis, Blinc, Lee, & Cox, 1995; Jin et al., 2012). Therefore, the development of new biodegradable and biocompatible nanometer-sized drug carriers is still urgent. These

* Corresponding author. Tel.: +86 931 8912387; fax: +86 931 8912582.
E-mail address: mzliu@lzu.edu.cn (M. Liu).

0144-8617/$ – see front matter © 2013 Elsevier Ltd. All rights reserved.
http://dx.doi.org/10.1016/j.carbpol.2013.04.013

nanoparticles have given much highlight as advanced vehicle of different kinds of drugs due to their advantages in terms of drug protection, transport and delivery (Panyam & Labhasetwar, 2003; Ravi Kumar, Bakowsky, & Lehr, 2004). With ultra-small size and biocompatibility, the nanoparticles can be transported through the blood circulation to remote body sites. These characteristics may favor the therapeutic applications in the delivery of thrombolitics for longer circulation time.

The objective of the current work is to prepare anionic starch nanospheres to explore the potential thrombolytic application of nanosphere-loaded NK. With negative charges, the nanospheres could not only enhance loading capacity of NK, but also can improve its stability, lengthen its circulation time and minimize the effect of hemorrhage. The anionic starch nano-spheres were prepared to load NK to overcome the above disadvantages. The nanoparticles were obtained by using inverse micro-emulsion crosslinking. The effects of preparing conditions, such as oil–water ratio, starch amount, surfactant content and crosslinking agent on starch nanospheres size were systematically studied. Besides, the morphology, cytotoxicity, biodegradability, and vitro thrombolytic behaviors of NK-loaded anionic starch nanospheres were also studied.

2. Experimental

2.1. Materials and methods

Soluble starch was purchased from Zhejiang linghu Chemical Reagent Factory, chemical purity grade. Span 80 and liquid paraffin were purchased from Fine Chemical Industry Institute of Tianjin Guangfu, chemical purity grade. Phosphoric trichloride ($POCl_3$) was of analytical purity grade and was provided by Shanghai Chemical Reagent Company of Chinese Medical Group. Sodium hydroxide (NaOH) was purchased from Xi'an Chemical Plant. NK was provided by Shanghai Shenggong Bioengineering Technology Service Co., Ltd. The other reagents were of analytical purity grade and used without further purification.

2.2. Preparation of starch-nanoparticles

Preparation of aqueous phase (W phase): 10 mg/mL of soluble starch solution was prepared and hydrolyzed in boiling water bath for 10 min, then ultrasonicated for 30 min, followed by adjusting the pH to 10 with 1 mol/L NaOH solution. Preparation of oil phase (O phase): 0.5 g of Span 80 was dissolved in 100 mL of paraffin in a beaker and stirred for 30 min in a 30 °C thermostated water bath. Then 10 mL of W phase was added dropwise into 100 mL of O phase under mechanical agitation of 1000 r/m. After 30 min, 30 μL of $POCl_3$ was added. The anionic starch nanospheres formed after 4 h. The emulsion was centrifuged and purified with distilled water and ethanol alternatively for several times. The obtained starch nanospheres was air-dried and suspended in alcohol, respectively, for further analysis and utilization.

2.3. FTIR analysis

IR absorption spectra of the samples were taken on a Fourier transform infrared (FTIR) spectrometer (Nicolet 670 FTIR, USA) over the region from 4000 to 400 cm^{-1}. The exhaustively dehydrated starch nanospheres were thoroughly ground with KBr powder prior to analysis, and pellets were prepared by compression under vacuum.

2.4. Starch-nanoparticle morphology by scanning electron microscope (SEM) images

The starch particles immersed in anhydrous alcohol were ultrasonicated for 15 min, followed by dropping the dispersions onto aluminum stubs and sputter-coated with gold for 300 s fractured, and the exterior morphology was examined with scanning electron microscope (SEM) (JSM-5600 LV SEM, Japan).

2.5. Transmission electron microscope (TEM) analysis

The morphologies and particle size of anionic starch nanospheres were characterized by a JEM-1200 EX/S transmission electron microscope (TEM). Before examination, the particles were dispersed in anhydrous alcohol and ultrasonicated for 15 min, and then deposited on a copper grid covered with a perforated carbon film.

2.6. Analysis of Z-potential

For *Z*-potential measurements, starch nanospheres ethanol dispersions with concentration of 1 g/L were ultrasonicated for 15 min prior to being transferred into dish. Zetasizer (2004, Malvern Instruments, U.K.) was used for measuring the distribution of the electrophoretic mobility of particles, the analyzer calculates the *Z*-potential from electrophoretic mobility using the Henry equation and Smolukowsky approximation. The isoelectric point corresponds to the point where potential value is zero, and all charges of particles are neutralized (Tan, Koopal, Weng, Vanriemsdijk, & Norde, 2008). Each sample was measured in triplicate at 20 °C.

2.7. Particle size measurements

Particle size of the obtained particles was recorded by a thermally controlled dynamic light scattering (DLS) at the scattering angle of 90° in alcohol using 90 Plus Particle Size Analyzer (Brookhaven Instruments Corporation) at room temperature. The particle size was determined as the maximum of the peak obtained in the CONTIN histogram. Further, the experimental data proved to give monomodal CONTIN histogram analyzed by the cumulants method giving access to some information on the *z*-average diffusion coefficient of the system. About 10 mg of starch particles were transferred into 10 mL anhydrous alcohol and ultrasonicated for 15 min to avoid the agglomeration of particles during measurements. The final particle diameter was calculated from a mean of at least three measurements.

2.8. Cytotoxicity assay

Cytotoxicity essay of anionic starch nanospheres was performed by 3-[4,5-dimethylthiazol-2-yl]-2,5-diphenyl tetrazolium bromide (MTT) assay using HeLa cells which grown in DMEM with 10% of fetal bovine serum (FBS) and were cultured in humidified atmosphere (5% CO_2, 37 °C). Then the cells were seeded into 96-well plates at a density of 7×10^3 cells/well, followed by incubating the plates at 37 °C for 4 h. Then, the original medium was replaced with 100 μL of fresh medium. Solution (10 μL) of nanospheres was sterilized by autoclave, and were injected into the 96-well plates, mixed, and incubated at 37 °C for 24 h. Next, the MTT reagent (10 μL in PBS, 5 mg/mL) was added to each well for further 4 h. Then, the medium was removed and 100 μL of DMSO was added to dissolve the formed formazan crystals. Untreated cells which were taken as control had 100% viability, and the cytotoxicity of nanoparticles was defined as the relative viability (%) which correlates

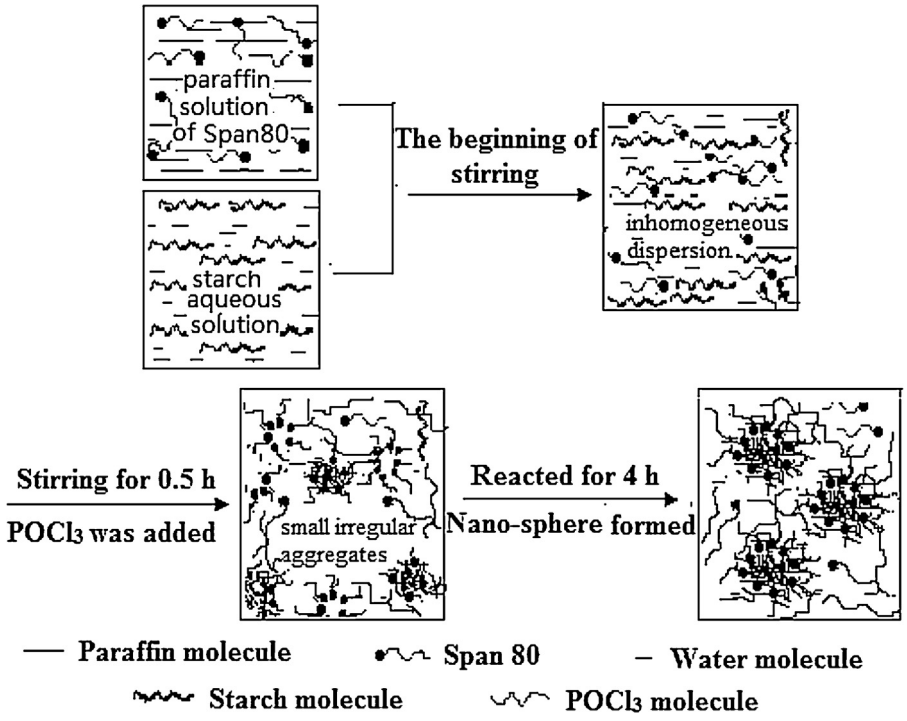

Fig. 1. A schematic representation of the main processes for preparing anionic starch nanosphere.

with amount of liable cells compared with cell control. The values reported were mean of three replicate.

2.9. Degradation test

The α-amylase solution (200 U/L) was prepared by PBS (pH = 7.4, I = 0.1). Then 35 mg of anionic starch nanospheres were dispersed in 35 mL of α-amylase solution, followed by dividing the solution into seven groups that were transferred into tubes. The degradation was performed at 37 °C, 2 mL of supernatant of one tube was take out at given time intervals to measure glucose content. Anionic starch nanospheres dispersed in PBS without α-amylase served as the control. Glucose content was determined with 3,5-dinitrosalicylic acid colorimetric method (DNS method) (Teixeira, Silva, Ferreira-Leitao, & Bon, 2012). The degradation ratio of starch nanospheres was calculated as follows:

$$W(\%) = \frac{M_{de}}{M_{st}} \times 100 \quad (1)$$

where M_{de} is the amount of degraded starch nanospheres and M_{st} is the total amount of starch nanospheres.

2.10. Vitro thrombolytic behavior study

Preparation of NK-loaded nanospheres. 100 mg of anionic starch nanospheres were suspended in 100 mL of NK PBS solution (0.1 mg/mL) for 2 days at 4 °C, followed by lyophilization to obtain the NK-loaded anionic starch nanospheres.

Vitro thrombolytic behavior study. The fresh chicken blood was obtained from vegetable market without any medication or hematological disease and placed at room temperature to form the clot. The clot was cut into parts in cylinder morphology (300–500 mm^3) which were transferred into tubes containing 20 mL of NK-loaded nanospheres PBS (1 mg/mL, pH = 7.4, I = 0.1). The thrombolytic behavior study was performed at 37 °C. The weights of blood clot were obtained after wiping off the excess surface water with filter paper at given time intervals. Moreover, free NK PBS (0.1 mg/mL, pH = 7.4, I = 0.1) and PBS (pH = 7.4, I = 0.1) served as controls. The clot mass loss ratio was calculated as follows:

$$W_{thr}(\%) = \frac{M_0 - M_t}{M_0} \times 100 \quad (2)$$

where M_0 is the amount of original clot, M_t is the amount of clot at time t.

3. Results and discussion

3.1. Synthesis of anionic starch nanospheres

In this work, reverse micro-emulsion crosslinking was used for synthesizing anionic starch nanospheres. Although, both $POCl_3$ and phosphate anions can introduce negative charge and contribute to the Z-potential decrease after crosslinking (Carbinatto, Castro, & Cury, 2012; Kim, Hwang, Kim, & Baik, 2012), while phosphate anions are powders, and much easier to adhere to the reactor wall and loss, while $POCl_3$ cannot loss. Thus, the liquid $POCl_3$ was chosen for crosslinker. The synthesizing schematic diagram of anionic starch nanospheres was showed in Fig. 1. Firstly, with magnetic stirring of 1000 r/min, liquid paraffin and Span 80 were mixed to form homogeneous and transparent system at 30 °C. Then, the W phase was dropped into the O phase, an inhomogeneous dispersion system formed after 0.5 h, followed by the addition of $POCl_3$. Meanwhile, the starch molecules began to aggregate, which was accompanied by crosslinking, then irregular aggregates. While a moiety of emulsion molecules aggregated themselves, other centralized around the starch aggregates. The small aggregates could be further crosslinked to larger sphere, and the water insoluble starch nano-sphere formed. The yield of starch nanospheres was about 75%.

3.2. FTIR analysis

Fig. 2A shows the FTIR spectra of soluble starch and anionic starch nanospheres crosslinked by $POCl_3$. As shown from the

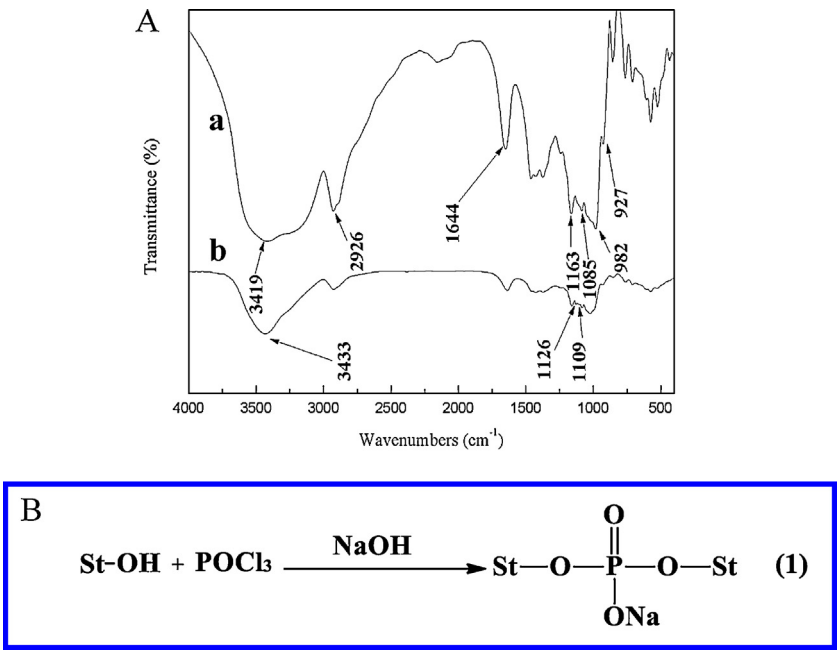

Fig. 2. (A) FTIR spectra of soluble starch (a) and anionic starch nanospheres crosslinked by $POCl_3$ (b). (B) The crosslinking reaction scheme of starch by $POCl_3$.

figure, native starch and starch nanospheres have different profiles. In the spectrum of native starch (Fig. 2A (a)), a broad band resulting from vibration of O–H appeared at 3419 cm^{-1}. The band around 2926 cm^{-1} is assigned to the C–H stretching vibration. The characteristic absorption band occurred at 1644 cm^{-1} were presumable originates from tightly bound water present in the starch molecules (Sung, Park, Choi, & Jhon, 2005). The characteristic absorption bands occurred in the fingerprint region at 1163, 1085, 982 and 927 cm^{-1}, respectively, were attributed to C–O bond stretching (Fang, 2004; Singh & Nath, 2011). Compared with native soluble starch, the spectrum of starch nanospheres shows new peaks at 1126 and 1109 cm^{-1}, as showed in Fig. 2A (b), which attributed to stretching vibration of P = O and P–O resulted from the crosslinking of $POCl_3$ (Simi & Emilia Abraham, 2007), respectively. Moreover, the vibration of O–H was red-shifted from 3419 to 3433 cm^{-1} due to the electron attracting group of P = O. All the data indicated that the starch nanospheres had been prepared successfully. In the alkaline systems, starch nanosphere was synthesized in the form of phosphate ester as showed in Fig. 2B.

3.3. Morphology of anionic starch nanospheres

Morphologies of soluble starch, starch nanospheres crosslinked and uncrosslinked are represented in Fig. 3. As showed in Fig. 3a, the native starch particles were irregular ellipse with a short diameter about of 30 μm and a long diameter about of 40 μm, while the starch nanosphere (feed composition: 0.5 g of soluble starch, water/oil was 1:5, 0.5 g of Span 80) were nearly spherical and with an average diameter of 150 nm, and exhibited a rough surface. Compared b and c, crosslinked starch nanospheres adhered each other slightly. The reason maybe that high crosslinking density corresponding to less free chains existed on the surface of starch nanospheres, thus, there are much weaker twisting effects due to the less free chains, then the particles adhered slightly. On the other hand, uncrosslinked starch nanospheres possessed poor mechanical strength and could deform more easily, which was beneficial to particle aggregation. Therefore, it is necessary to crosslink for preparing starch nanospheres with more stable shape and better dispersity.

3.4. TEM analysis

The TEM images of the anionic starch nanospheres prepared under different conditions are shown in Fig. 4. As can be seen, most of the starch nanoparticles have a good sphericity and the particle size ranges from 20 to 400 nm. Compared to other particles suspended in alcohol, the particles air-dried for 3 months (Fig. 4a) appeared to have evidently clear outline, which attributed to deswelling effect. The size of starch nanospheres exhibited an increasing trend as starch content increased from 0.2 (Fig. 4b) to 0.5 g (Fig. 4c) and 1.0 g (Fig. 4d). The particle size decreased from 130 nm (Fig. 4b) to 90 nm (Fig. 4e) as Span 80 content increased from 0.5 to 1.5 g. The more the emulsifier, the smaller the surface tension of the droplets, leads to a smaller particle size. When crosslinker decreased to 1 μL, starch particles increased to 150 nm (Fig. 4f). Moreover, the particles appeared to be core/shell structure, the reason may be that the very few crosslinker during the later reaction leaded to a quite lower crosslinking density. The TEM image of the particles prepared under oil/water (O/W) ratio of 10:1 (v/v) is shown in Fig. 4g. Particle size was reduced to 60 nm, which can be explained by power input theory (Shi, Li, Wang, Li, & Adhikari, 2011). The other possible reason is that when increasing the O/W ratio, there would be relatively less emulsifier.

3.5. Z-potential analysis

The zeta potentials of anionic starch nanospheres prepared under different $POCl_3$ content were measured. As the mole ratio of $POCl_3$ to starch units varies from 3.4% to 10.2%, the samples were named with $Particle_{3.4}$, $Particle_{5.1}$, $Particle_{6.8}$, $Particle_{8.5}$, and $Particle_{10.2}$, respectively. As illustrated in Table 1, all of the starch nanospheres possessed negative *Z*-potential. Based on this property, the particles could be used for loading or adsorption for electropositive molecule, combined with their biocompatibility and biodegradability, the starch nanospheres could have good application prospects in many fields. As also can be seen, the *Z*-potential decreased with the increase of $POCl_3$ content. Because $POCl_3$ could bring negative charge after crosslinking, thus,

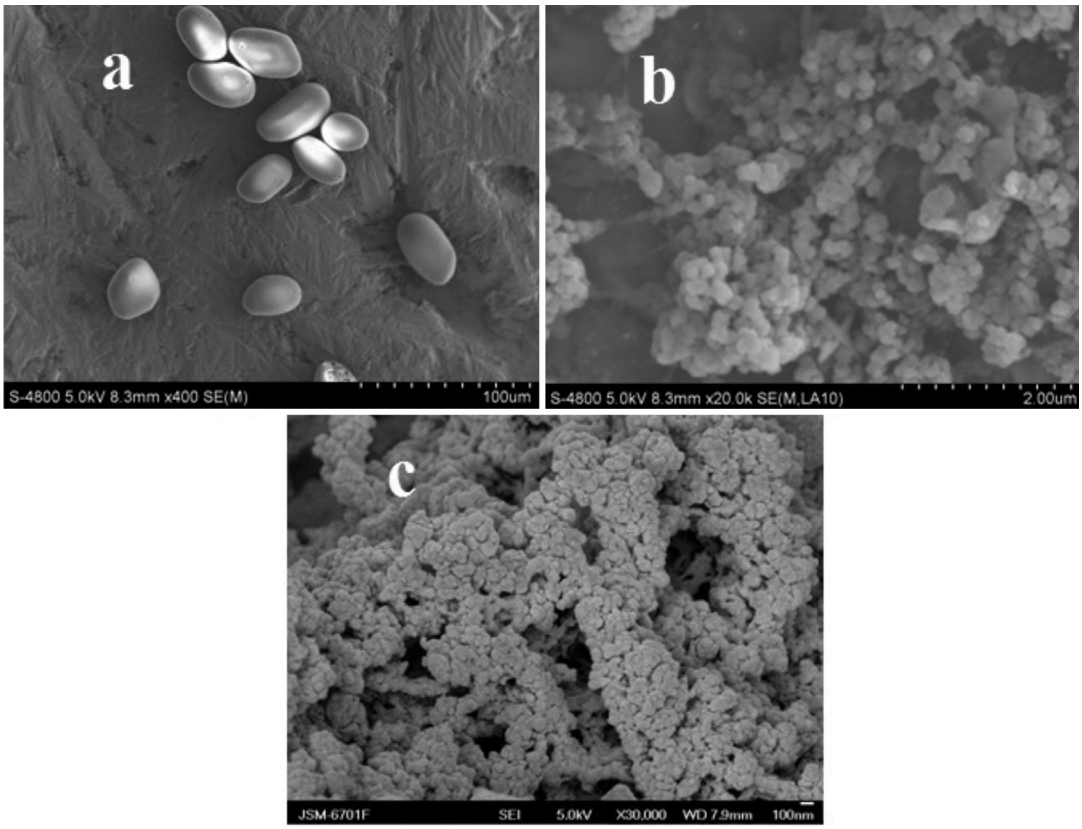

Fig. 3. SEM images of (a) native soluble starch, (b) crosslinked starch nanospheres and (c) uncrosslinked starch nanospheres.

an increase of 6.46% in $POCl_3$ content could lead to an eventual decrease of 148 mV in *Z*-potential. Another reason may be that a higher crosslinking density results in a smaller particle size which corresponded to a lower *Z*-potential (Romero-Pérez, García-García, Zavaleta-Mancera, & Ramírez-Bribiesca, 2010). When the mole ratio of $POCl_3$ was more than 6.80%, the *Z*-potential is basically stable due to the saturated crosslinking density.

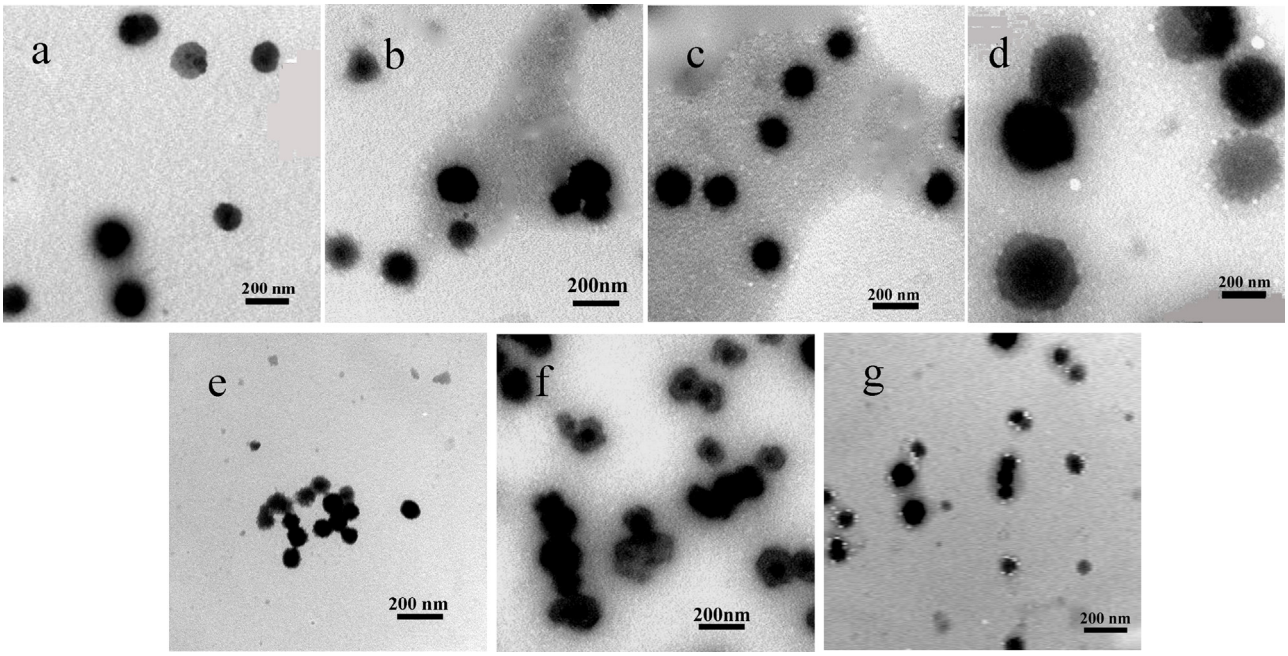

Fig. 4. TEM images of the starch nanospheres prepared under different conditions. (a) Starch: 0.2 g, oil/water: 5:1, Span 80: 0.5 g, $POCl_3$: 30 μL, air-dried; (b) starch: 0.2 g, oil/water: 5:1, Span 80: 0.5 g, $POCl_3$: 30 μL, suspended in alcohol; (c) starch: 0.5 g, oil/water: 5:1, Span 80: 0.5 g, $POCl_3$: 30 μL, suspended in alcohol; (d) starch: 1.0 g, oil/water: 5:1, Span 80: 0.5 g, $POCl_3$: 30 μL, suspended in alcohol; (e) starch: 0.2 g, oil/water: 5:1, Span 80: 1.5 g, $POCl_3$: 30 μL, suspended in alcohol; (f) starch: 0.2 g, oil/water: 5:1, Span 80: 0.5 g, $POCl_3$: 1 μL, suspended in alcohol; (g) starch: 0.2 g, oil/water: 10:1, Span 80: 0.5 g, $POCl_3$: 30 μL, suspended in alcohol.

Table 1
Feed compositions for the preparation of starch nanospheres and the effect of $POCl_3$ content on *Z*-potential nano-starch.

	$Particle_{3.4}$	$Particle_{5.1}$	$Particle_{6.8}$	$Particle_{8.5}$	$Particle_{10.2}$
$POCl_3$ (Mr%)[a]	3.4	5.1	3.4	8.5	10.2
Soluble starch (g)	0.5	0.5	0.5	0.5	0.5
Liquid paraffin (mL)	100	100	100	100	100
Distilled water (mL)	20	20	20	20	20
Span 80 (g)	0.5	0.5	0.5	0.5	0.5
Z-potential (mV)	−85	−132	−136	−233	−239

[a] The mole ratio of $POCl_3$ based on the amount of starch structure units.

3.6. Optimization for preparation of anionic starch nanospheres

The normal composition feed as follows: starch, 0.2 g; O/W, 5:1; Span 80, 0.5 g; $POCl_3$, 30 μL. During every optimization of starch nanospheres, only one condition was changed, the other components were same as the normal composition feed. For example, in starch content optimization, only starch content was changed from 0.2 g to 2.0 g, the other components were same as the normal composition: O/W, 5:1; Span 80, 0.5 g; $POCl_3$, 30 μL, under no air-dried condition.

3.6.1. Effect of soluble starch concentration

The effect of soluble starch content on particle size was studied. The corresponding size of starch nanospheres with increasing soluble starch content is presented in Fig. 5a. A remarkable increase of particle size can be seen as starch content increased, which could be explained by decreasing crosslinking intensity resulted from increasing concentration of starch content. On the other hand, reaction time could reflect the crosslinking intensity and the apparent cross-linking kinetics, thus, the reaction time may affect the viscosity of both W phase and the emulsion. While the viscosity variation means that the emulsion process required various level of energy input to from the miniemulsions which eventually resulted in variation in particle size.

3.6.2. The effect of surfactant content

Fig. 5b shows the effect of Span 80 content on the nanosphere size. As can be seen, the nanoparticles size is affected by the increasing surfactant content quite significantly (Zaragoza-Contrerasa & Navarro-Rodríguez, 2003). Evidently, the particle size showed a decreasing trend when Span 80 content increased from 0.2 to 1.5 g and maintained a constant when Span 80 content was more than 1.5 g. The possible explanation for this phenomenon has been provided by 'The optimal amount' theory (Jose, 2002; Landfester, 2002; Niemann & Sundmacher, 2010). According to the theory, certain amount of surfactant optimally covered the surface of the droplets and provided the maximum stability against droplet coalescence, which leading to the smallest emulsion size. If the surfactant was not enough to completely cover the droplets after homogenization process, the droplets would tend to aggregate with each other to reduce the surface area. On the contrary, when the surfactant content was excess, the free surfactant molecules will ultimately adhere to the droplets, which results in the increase in the droplets size. Nevertheless, the excess amount of surfactant would be cleared during the post processing, thus, it could not affect the particle size. These results indicated that the nanoparticles would be the smallest under optimal surfactant concentration.

3.6.3. Effect amount of crosslinker

Various starch nanospheres were prepared under different crosslinker amount to study the effect on the particle size, and the result is shown in Fig. 5c. As can be seen, the particle size was significantly affected by the $POCl_3$ amount and showed a decreased trend with increasing $POCl_3$ amount at the beginning, and tended to be constant at last. When the starch amount, O/W ratio and surfactant content were same, the amount and size of every droplet was equivalent, moreover, the starch content within every droplet was equal to each other. While much more crosslinker would lead to a quite higher crosslinking density, and resulted in a tightly interaction between starch molecules, then the particle size decreased. While, the crosslinking density became saturation as $POCl_3$ continued to be added, leading to constant trend of particle size.

3.6.4. Effect of the oil/water ratio

The effect of O/W ratio on the particle size of anionic starch nanospheres can be observed in Fig. 5d. Evidently, the particle size appeared to decrease from 154 to 93 nm as O/W increased from 5 to 10. The possible reason may be that when the W phase volume decreased, lower power input would be required to increase the droplet size during the emulsification process (Constantinides, Lancaster, & Marcello, 1995). When O/W increased, the droplets became smaller under the same energy level, which eventually leaded to the increase in the starch nanosphere size. The other possible reason was that when decreasing O/W, there would be relatively more emulsifier, which resulted in a lower surface tension of the droplets, leading to a smaller particle size (Sajjadi, Zerfa, & Brooks, 2003). However, when O/W was more than 10, the particle size had a marked increase with increasing O/W, and no constant trend appeared. The reason may be that the little water was not enough to dissolve the same amount of starch thoroughly, although it could change the original starch size, the undissolved starch particles were reserved after the whole reaction, and thus, a larger anionic starch nanosphere size was obtained.

3.7. Cytotoxicity test and degradation analysis

Cytotoxicity assay was conducted to study the cytotoxicity of the anionic starch nanosphere by varying its concentration via MTT assay. The results were displayed in Fig. 6A. The results demonstrate that, after 48 h, in all the concentrations studied, the nanospheres did not present obvious cytotoxicity to the cells. For example, even for the maximum concentration, the cell viability was 88%. Therefore, the anionic starch nanospheres are biocompatible, which is important for biomaterials.

DNS method (Teixeira et al., 2012) was employed to study the degradation of anionic starch nanospheres, and the result was shown in Fig. 6B. In Fig. 6B, a showed the degradation behavior of the nanospheres in α-amylase solution (200 U/L) whose concentration is close to that (40–180 U/L) in serum, and b was the PBS control without α-amylase. Evidently, the particles in α-amylase solution degraded much faster than that without α-amylase. The W of the nanospheres with α-amylase reached about 55% after 4 days and 84% when degradation performed for 7 days. While as for the control, 22% of the nanospheres degraded after 4 days and only 47% degraded in one week. The good degradation behaviors in blood circulation system make these systems potential drug carriers.

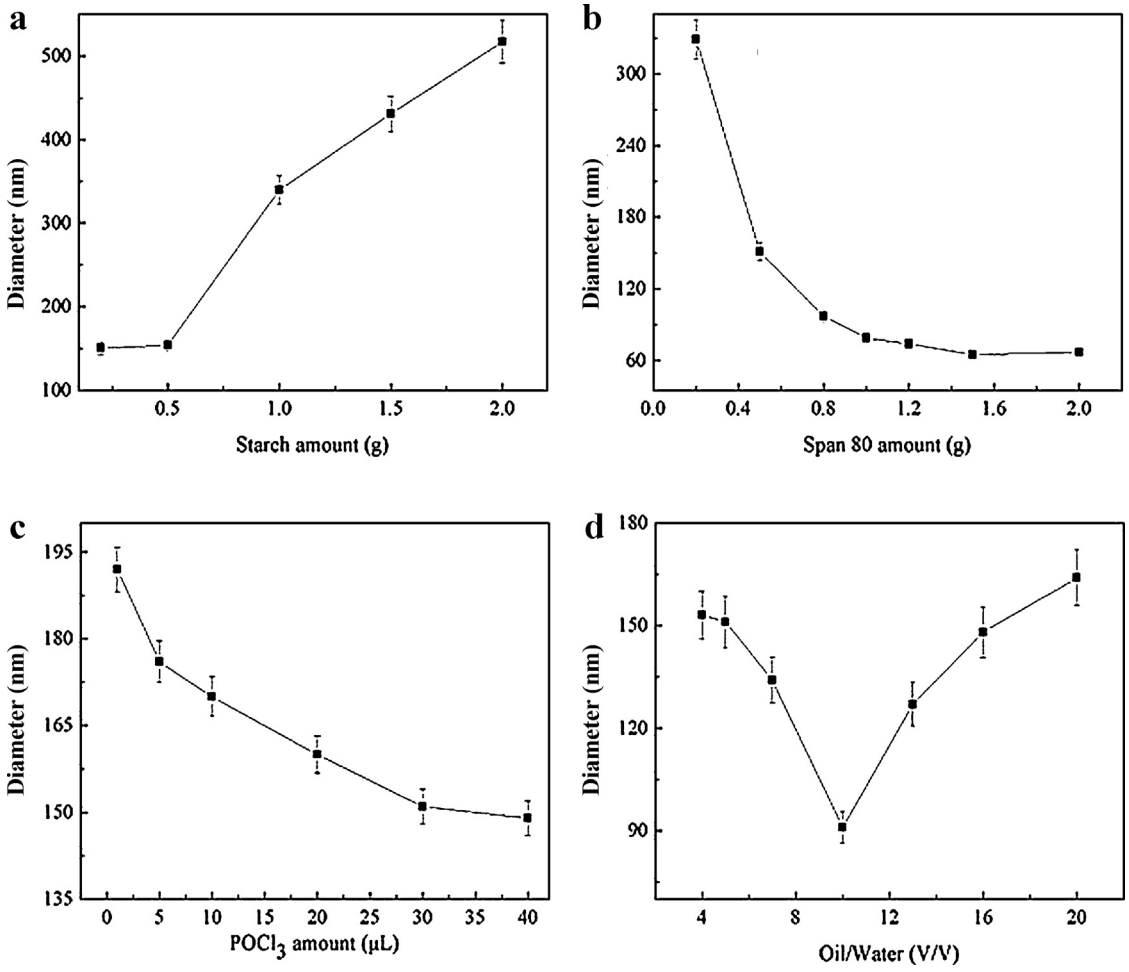

Fig. 5. Optimization of nanoparticle formulation: (a) Starch amount; (b) Span 80 amount; (c) $POCl_3$ amount; (d) oil/water.

3.8. Thrombolytic behavior analysis

The thrombolytic behavior of starch nanoparticles loaded NK (NP-loaded NK), original starch loaded NK (OS-loaded NK), free NK and saline were shown in Fig. 7. As can be seen from Fig. 7A, in the first 2.5 h of incubation, 22 and 25 wt% of the clots was dissolved by nude NK and OS-loaded NK, respectively. Whereas it was 15 wt% by the nanospheres containing equivalent amount of NK, and almost 0 wt% for saline, which demonstrate that the thrombolytic rate of NK loaded the nanospheres keeps at slower rate. The photograph in Fig. 7A shows thrombolytic degree of the two clots in NP-loaded and nude NK solutions after 0.5 h, respectively. Evidently, nude NK resulted in a higher thrombolytic rate implied by the deeper color, which further demonstrates the above conclusion. NK encapsulation by the nanospheres via electrostatic interaction will not only benefit the protection of NK from fast biodegradation

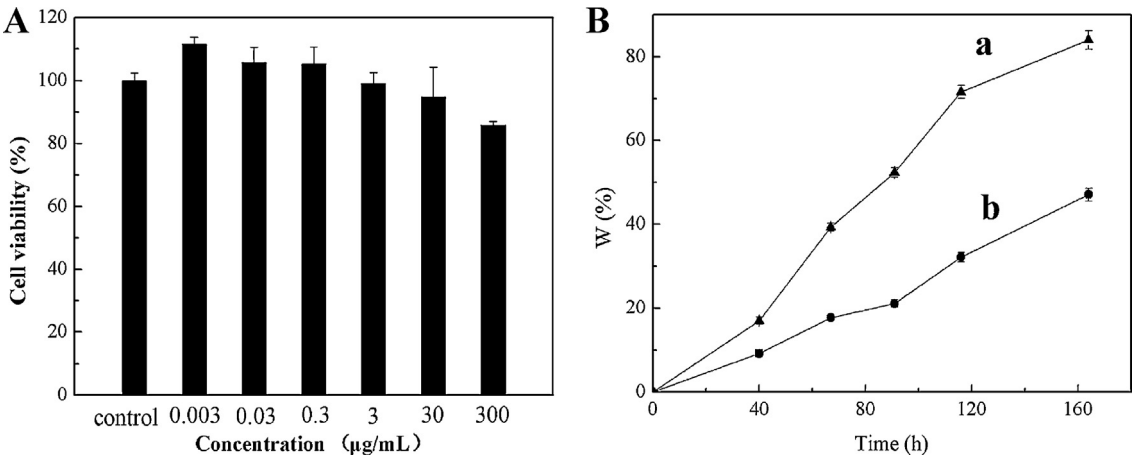

Fig. 6. (A) Cytotoxicity test on Hela cells at different particles concentrations (0.003, 0.03, 0.3, 3, 30, 300 μg/mL, $n = 3$). (B) Degradation test (a: with α-amylase, b: without α-amylase).

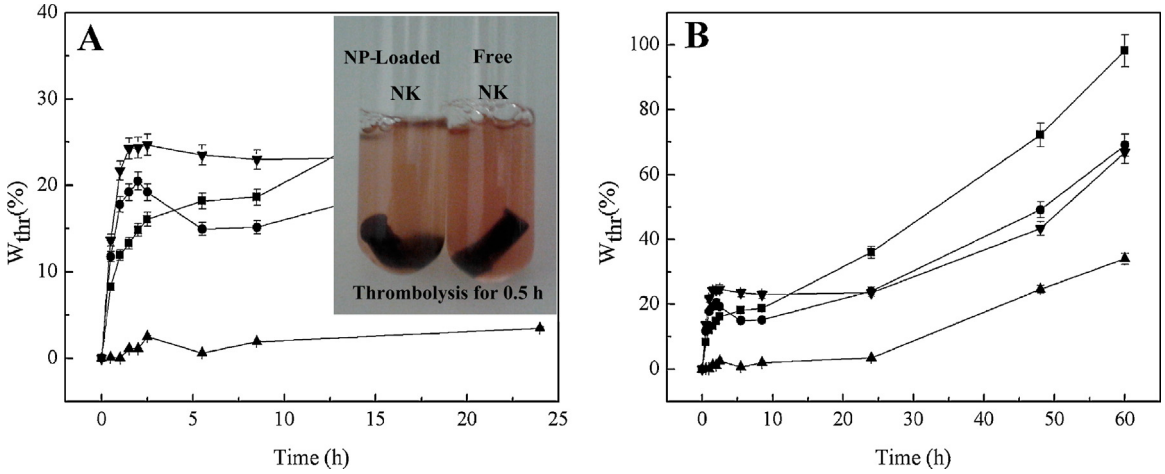

Fig. 7. Thrombolytic behaviors of anionic starch nanosphere (A: 24 h; B: 60 h. ■: NP-loaded NK; ●: free NK; ▼: OS-loaded NK; ▲: saline).

hence prolongs the circulation in vivo, but also can significantly reduce the risk of acute hemorrhage complication by decreasing the thrombolysis rate. Moreover, the ultra-small carriers could inhibit the immunology response from the reticuloendothelial system (Hu et al., 2003; Kim, Kim, Park, Byun, & Kim, 2009). The W_{thr} of the clot in nude NK and solution decreased more than 2.5 h, which is constant with the trend of that in saline solution. On the one hand, most of the nude NK is easy to become deactivation at 37 °C, leading to a decreased thrombolytic rate. On the other hand, clot could swell in water, which caused an increased clot mass. The control of OS-loaded NK showed a quite similar trend as the nude NK, because original starches carry no negative charge, it has a poor interaction with NK, which leading to the bareness of most of the NK. Whereas, W_{thr} of the clot in NP-loaded NK nanospheres solution still showed a rising trend due to NK protection and delivery by anionic starch nanospheres via hydrogen bond and electrostatic interaction. When time was prolonged to 60 h, as shown in Fig. 7B, the mass of the four clots decreased gradually resulted from fibrin's own hydrolysis. Differently, the clot dissolved by the NP-loaded NK solution showed a faster thrombolytic rate due to protected and controlled released NK. In conclusion, the anionic starch nanospheres can improve stability of NK, lengthen its circulation time and minimize the effect of hemorrhage.

4. Conclusions

This paper is considered as the first report on the investigation of NK release from anionic starch nanospheres. It has prepared ultra-small and anionic starch nanospheres. Non-toxic liquid paraffin was used as O phase and $POCl_3$ was used as crosslinker to introduce negative charge to load NK possessing a *pI* of 7.8. Optimizations of preparation conditions demonstrated that the anionic starch nanosphere with quite small size of 26 nm can be obtained under an appropriate condition. The cytotoxicity and biodegradability studies demonstrated that the anionic starch nanospheres are non-toxic, biocompatible and biodegradable. Vitro thrombolytic behaviors for NK-loaded anionic starch nanospheres indicated that the drug-particles possess a better thrombolytic behavior and could avoid hemorrhage.

Acknowledgements

The authors gratefully the financial support of the Special Doctorial Program Fund of the Ministry of Education of China (grant no. 20090211110004) and the Fund for Train Men for profession of National Natural Science Foundation of China (grant no. J1103307).

References

Angellier, H., Molina-Boisseau, S., & Dufresne, A. (2005). Mechanical properties of waxy maize starch nanocrystal reinforced natural rubber. *Macromolecules*, *38*(22), 9161–9170.
Brekenfeld, C., Remonda, L., Nedeltchev, K., Arnold, M., Mattle, H. P., Fischer, U., et al. (2007). Symptomatic intracranial haemorrhage after intra-arterial thrombolysis in acute ischaemic stroke: Assessment of patients treated with urokinase. *Journal of Neurology, Neurosurgery & Psychiatry*, *78*(3), 280–285.
Carbinatto, F. M., Castro, A. D., & Cury, B. S. F. (2012). Physical properties of pectin–high amylose starch mixtures cross-linked with sodium trimetaphosphate. *International Journal of Pharmaceutics*, *423*(3), 281–288.
Chen, G., Wei, M., Chen, J., Huang, J., Dufresne, A., & Chang, P. R. (2008). Simultaneous reinforcing and toughening: New nanocomposites of waterborne polyurethane filled with low loading level of starch nanocrystals. *Polymer*, *49*(7), 1860–1870.
Constantinides, P. P., Lancaster, C. M., & Marcello, J. (1995). Enhanced intestinal absorption of an RGD peptide from water in oil microemulsions of different composition and particle size. *Journal of Controlled Release*, *34*(3), 109–116.
Erdoğan, S., Özer, A. Y., & Bilgili, H. (2005). In vivo behaviour of vesicular urokinase. *International Journal of Pharmaceutics*, *295*(1–2), 1–6.
Fang, J. (2004). The chemical modification of a range of starches under aqueous reaction conditions. *Carbohydrate Polymers*, *55*(3), 283–289.
Francis, C. W., Blinc, A., Lee, S., & Cox, C. (1995). Ultrasound accelerates transport of recombinant tissue plasminogen activator into clots. *Ultrasound in Medicine & Biology*, *21*(3), 419–424.
Hu, Y., Jiang, X., Ding, Y., Zhang, L., Yang, C., Zhang, J., et al. (2003). Preparation and drug release behaviors of nimodipine-loaded poly(caprolactone)–poly(ethylene oxide)–polylactide amphiphilic copolymer nanoparticles. *Biomaterials*, *24*(13), 2395–2404.
Jin, H., Tan, H., Zhao, L., Sun, W., Zhu, L., Sun, Y., et al. (2012). Ultrasound-triggered thrombolysis using urokinase-loaded nanogels. *International Journal of Pharmaceutics*, *434*(1–2), 384–390.
Jobling, S. (2004). Improving starch for food and industrial applications. *Current Opinion in Plant Biology*, *7*(2), 210–218.
Jose, M. A. (2002). Miniemulsion polymerization. *Progress in Polymer Science*, *27*(5), 1283–1346.
Kim, J. Y., & Lim, S. T. (2009). Preparation of nano-sized starch particles by complex formation with n-butanol. *Carbohydrate Polymers*, *76*(1), 110–116.
Kim, J. Y., Kim, J. K., Park, J. S., Byun, Y., & Kim, C. K. (2009). The use of PEGylated liposomes to prolong circulation lifetimes of tissue plasminogen activator. *Biomaterials*, *30*(29), 5751–5756.
Kim, H., Hwang, D., Kim, B., & Baik, M. (2012). Cross-linking of corn starch with phosphorus oxychloride under ultra high pressure. *Food Chemistry*, *130*(7), 977–980.
Kristo, E., & Biliaderis, C. G. (2007). Physical properties of starch nanocrystal-reinforced pullulan films. *Carbohydrate Polymers*, *68*(1), 146–158.
Landfester, M. A. K. (2002). Polyreactions in miniemulsions. *Progress in Polymer Science*, *27*(3), 689–757.
Le Corre, D., Bras, J., & Dufresne, A. (2010). Starch nanoparticles: A review. *Biomacromolecules*, *11*(5), 1139–1153.
Li, Y. J., & Ni, Y. M. (2004). Removal of Cu(II) from aqueous solutions by chelating starch derivatives. *Journal of Applied Polymer Science*, *92*(7), 3881–3885.
Ma, X. F., Peter, R., & Yu, J. G. (2008). Fabrication and characterization of citric acid-modified starch nanoparticles/plasticized-starch composites. *Biomacromolecules*, *9*(12), 3314–3320.

Niemann, B., & Sundmacher, K. (2010). Nanoparticle precipitation in microemulsions: Population balance model and identification of bivariate droplet exchange kernel. *Journal of Colloid Interface Science*, *342*(2), 361–371.
Panyam, J., & Labhasetwar, V. (2003). Biodegradable nanoparticles for drug and gene delivery to cells and tissue. *Advanced Drug Delivery Reviews*, *55*(4), 329–347.
Polaczek, E. F. S., Malenki, K., & Tomasik, P. (2000). Inclusion complexes of starches with hydrocarbons. *Carbohydrate Polymers*, *43*(1), 291–297.
Ravi Kumar, M. N. V., Bakowsky, U., & Lehr, C. M. (2004). Preparation and characterization of cationic PLGA nanospheres as DNA carriers. *Biomaterials*, *25*(10), 1771–1777.
Romero-Pérez, A., García-García, E., Zavaleta-Mancera, A., & Ramírez-Bribiesca, J. E. (2010). Designing and evaluation of sodium selenite nanoparticles in vitro to improve selenium absorption in ruminants. *Veterinary Research Communications*, *34*(1), 71–79.
Sajjadi, S., Zerfa, M., & Brooks, B. W. (2003). Phase inversion in p-xylene/water emulsions with the non-ionic surfactant pair sorbitan monolaurate/polyoxyethylene Sorbitan monolaurate (Span 20/Tween 20). *Colloids and Surfaces A*, *218*(2), 241–254.
Shi, A. M., Li, D., Wang, L. J., Li, B. Z., & Adhikari, B. (2011). Preparation of starch-based nanoparticles through high-pressure homogenization and miniemulsion cross-linking: Influence of various process parameters on particle size and stability. *Carbohydrate Polymers*, *83*(4), 1604–1610.
Simi, C. K., & Emilia Abraham, T. (2007). Hydrophobic grafted and cross-linked starch nanoparticles for drug delivery. *Bioprocess Biosystems Engeering*, *30*(3), 173–180.
Singh, A. V., & Nath, L. K. (2011). Synthesis and evaluation of physicochemical properties of cross-linked *Phaseolus aconitifolius* starch. *Starch*, *63*(10), 655–660.
Song, D., Zhao, Y., Dong, C., & Deng, Y. (2009). Surface modification of cellulose fibers by starch grafting with crosslinkers. *Journal of Applied Polymer Science*, *113*(5), 3019–3026.
Song, D., Thio, Y. S., & Deng, Y. (2011). Starch nanoparticle formation via reactive extrusion and related mechanism study. *Carbohydrate Polymers*, *85*(1), 208–214.
Sung, J. H., Park, B. J., Choi, H. J., & Jhon, M. S. (2005). Phosphorylation of potato starch and its electrorheological suspension. *Biomacromolecules*, *6*(4), 2182–2188.
Tan, W., Koopal, L., Weng, L., Vanriemsdijk, W., & Norde, W. (2008). Humic acid protein complexation. *Geochimica et Cosmochimica Acta*, *72*(8), 2090–2099.
Teixeira, R. S., Silva, A. S., Ferreira-Leitao, V. S., & Bon, E. P. (2012). Amino acids interference on the quantification of reducing sugars by the 3,5-dinitrosalicylic acid assay mislead carbohydrase activity measurements. *Carbohydrate Research*, *363*(1), 33–37.
Thielemans, W., Belgacem, M. N., & Dufresne, A. (2006). Starch nanocrystals with large chain surface modifications. *Langmuir*, *22*(10), 4804–4810.
Valodkar, M., & Thakore, S. (2011). Organically modified nanosized starch derivatives as excellent reinforcing agents for bionanocomposites. *Carbohydrate Polymers*, *86*(3), 1244–1251.
Zaragoza-Contrerasa, E. A., & Navarro-Rodríguez, D. (2003). On the role of an unconventional rigid rodlike cationic surfactant on the styrene emulsion polymerization. Kinetics, particle size and particle size distribution. *Polymer*, *44*(8), 5541–5546.